# Accelerated adaptive surrogate based optimization through reduced order modeling

Moindze Soilahoudine[1], Christian Gogu[2], Christian Bes[3]
*Université de Toulouse, UPS, INSA, Mines Albi, ISAE ; ICA (Institut Clément Ader),31062 Toulouse, France*

**The efficient global optimization (EGO) approach was often used to reduce the computational cost in the optimization of complex engineering systems. This algorithm can remain however expensive for large scale problems since each simulation uses the full numerical model. We propose a novel optimization approach for such problems, where the numerical model solves partial differential equations involving the resolution of a large system of equations, such as by finite element. Our method is based on the combination of the efficient global optimization (EGO) approach and reduced basis modeling. The novel idea is to use inexpensive, sufficiently accurate reduced basis solutions to significantly reduce the number of full system resolutions. Two applications of the proposed surrogate based optimization approach are presented: an application to the problem of stiffness maximization of laminated plates and an application to the problem of identification of orthotropic elastic constants from full-field displacement measurements based on a tensile test on a plate with a hole. Compared to the crude EGO algorithm, a significant reduction in computational cost was achieved using the proposed efficient reduced basis global optimization**.

## I. Introduction

One of the issues in many approaches for solving nonlinear optimization problems is that they often require a large number of function evaluations, with significant computational cost per evaluation. One way of reducing the computational cost is by using surrogates, also known as metamodels or response surface approximations to

[1] Ph.D. Student, UPS, INSA, Mines Albi, ISAE; ICA (Institut Clément Ader); 3 Rue Caroline Aigle, F-31400 Toulouse; S.moindze@gmail.com.
[2] Associate Professor, UPS, INSA, Mines Albi, ISAE; ICA (Institut Clément Ader); 3 Rue Caroline Aigle, F-31400 Toulouse; christian.gogu@gmail.com.
[3] Professor, UPS, INSA, Mines Albi, ISAE; ICA (Institut Clément Ader); Bât 3R1, 118 Route de Narbonne, F-31062 Toulouse; christian.bes@univ-tlse3.fr.

replace the expensive computational simulations [1–3]. Within the optimization domain, surrogate based optimization (a class of optimization methodologies that make use of surrogate modeling techniques to quickly find the local or global optima)[4–9] often progresses in cycles. Each cycle consists of constructing an approximation of the simulation response based on a limited number of runs of the expensive simulation, using the surrogate to search for a candidate for the next simulations, and finally analyzing the design. Multiple surrogate types can be used for fitting the samples, such as polynomial response surface approximations [10], neural networks [11–13], support vector machines [14–17].The efficient global optimization (EGO) [18] uses a surrogate uncertainty estimator to guide the selection of the next point (the point that maximizes the expected improvement) at which a simulation will be carried out. However, this algorithm can remain expensive because each simulation uses the full numerical model, which can itself be very expensive. Obtaining full numerical accuracy may however not be required during the optimization process as have shown [19,20]. For example, in areas that are far from the present best point a rough estimate of the solution may be sufficient to clarify the behavior of the objective function in this vicinity. Calculating a full numerical simulation at this point would thus be overkill in most situations. Instead, it would be advantageous if the optimization algorithms could adaptively select the level of fidelity it needs for the next sampling point and each new point would be thus calculated accordingly.

Besides progress in optimization algorithms, reduced order modeling approaches [21–23], by projection of the response on a reduced basis have proved to be efficient methods for achieving drastic dimensionality and computational cost reductions. The main idea behind this concept is to construct a so called reduced basis, and then solve the problem projected on this low dimensional basis with drastically reduced computational cost.

Reduced basis models have been applied before in the context of shape optimization [24] and topology optimization [25]and showed potential for improving the efficiency of the corresponding methods. To our best knowledge, they have not been applied to surrogate based optimization approaches that adaptively enrich the surrogate to solve global optimization problems.

The aim of this article is to propose a new surrogate based optimization approach for certain types of global optimization problems. Our approach is based on an adaptive coupling of the EGO algorithm with reduced basis modeling. The basic idea is that a reduced basis model may be sufficiently accurate for points that are much worse than the present best sample (exploration points) and for points near already computed solutions (exploitation points). A specific method for implementing this idea and constructing the reduced basis integrated with the kriging based optimization process is proposed. The corresponding approach can be seen as a multi-

fidelity optimization. Compared to existing multi-fidelity optimization approaches based on kriging or co-kriging [26–28] our proposed method can be seen as a tunable fidelity approach, since it tunes the fidelity of the reduced basis model to the accuracy requirements of the optimization.

The rest of the article is organized as follows. We provide in section II the problem statement. In section III we provide an overview of surrogate based optimization, efficient global optimization and reduced basis modeling. In section IV we describe the proposed framework for coupling reduced basis modeling with surrogate based optimization and provide three possible implementation algorithms: the key point efficient reduced basis global optimization (KPERBGO), the key point efficient reduced basis global optimization with terminal enrichment (KPERBGOTE) and the key point efficient co-kriging based global optimization (KPERCGO) algorithms. In section V we give a first application example of the proposed algorithm to the stiffness maximization of laminated plates. In section VI we give a second application example of the proposed algorithms to the identification of orthotropic elastic constants from full field displacement measurements based on a tensile test with a hole. Finally, we provide concluding remarks in section VII.

## II. Problem statement

Complex phenomena are modeled by complex mathematical models, implemented in large computer codes having significant computational cost. A single run of this computationally expensive code may take many hours. The computational cost issue is further amplified in optimization procedures requiring a large number of simulation runs and where the objective function may have a number of local minima.

We consider here optimization problems that need to make expensive numerical simulation calls and involve solving partial differential equations (by techniques such as the finite element method).

The global optimization problems considered in this work has the following form:

$$\begin{aligned} &\min_{\mu} f_{obj}(\boldsymbol{u};\ \boldsymbol{\mu}) \\ &K(\boldsymbol{\mu})\boldsymbol{u} = \boldsymbol{F} \\ &\boldsymbol{\mu}_i^l \le \boldsymbol{\mu}_i \le \boldsymbol{\mu}_i^u\ ,\ \ i = 1,2,..,p \end{aligned} \tag{1}$$

where:

- $\boldsymbol{u} \in \mathbb{R}^n$ the vector of state variables (e.g. the vector of nodal displacements in structural mechanics)
- $\mu \in \mathbb{R}^p$ is the set of parameter of interest (e.g. material properties)
- $\boldsymbol{\mu}_i^l \ and \ \boldsymbol{\mu}_i^u$ are given lower and upper bounds of the i$^{th}$ parameter.

- The equality constraint $K(\boldsymbol{\mu})\boldsymbol{u} = \boldsymbol{F}$ represents the satisfaction of the discretized equilibrium equations (resulting from a finite elements scheme for example) of the underlying physical phenomenon. $\boldsymbol{F}$ is a given vector of dimension *n* and for a given parameter of interest μ, $K(\boldsymbol{\mu})$ is a *n* x *n* matrix. Let us assume that for any value $\boldsymbol{\mu} \in \mathbb{R}^p$, $K^{-1}(\boldsymbol{\mu})$ is nonsingular. That is, there exists a unique solution $\boldsymbol{u}(\boldsymbol{\mu}) \in \mathbb{R}^n$ such that

$$K(\boldsymbol{\mu})\boldsymbol{u} = \boldsymbol{F} \qquad (2)$$

For example in structural mechanics $K(\boldsymbol{\mu})\boldsymbol{u} = \boldsymbol{F}$ represents the equations of the static equilibrium where $K(\boldsymbol{\mu})$ is the stiffness matrix, depending of materials properties $\boldsymbol{\mu}$ and $\boldsymbol{F}$ the vector of the applied forces. Note that while the problem is linear in $\boldsymbol{u}$, it is not necessarily linear in $\boldsymbol{\mu}$.

- $f_{obj} : \mathbb{R}^n \times \mathbb{R}^p \to \mathbb{R}$ is the objective function which represents a target to be optimized with respect to parameter $\boldsymbol{\mu}$. The objective function is generally non-linear and non-convex, possibly involving multiple local minima. For example $f_{obj}$ can be the strain energy or a least square objective function in identification problems.

For large scale problem both the computational time of computing the objective function $f_{obj}(.,.)$ and the factorization of the matrix $K(\boldsymbol{\mu})$ ,to solve the system of equations, can be quite expensive. In those cases direct uses of iterative optimization methods are not appropriate.

In the next section we provide an overview of some existing approaches for dealing with the computational cost issue of the optimization problem defined in (1). In particular we give an overview of surrogate based optimization and describe the EGO algorithm for dealing with the computationally expensive objective function. We then also present reduced basis modeling for dealing with computationally expensive numerical models. Finally, we will propose a new method combining EGO and the reduced basis approach.

## III. Surrogate based optimization and reduced basis modeling

### A. Surrogate-based optimization

Surrogate models, also known as metamodels or response surface models, are often used in place of the actual simulation code to find the local or global optimum and reduce the computational cost. The surrogate model can be regarded as an approximation of the objective function, which is built from a set of points called a design of experiment. The design of experiment and the corresponding simulations are used to construct a simpler mathematical model thus replacing the expensive model.

The readers are referred to [29–33], for more extensive description of surrogate modeling techniques, design of experiment and identification of new sampling points. An overview of the most popular methods in design space

sampling, surrogate model construction, model selection and construction and surrogate based optimization can be found in [4,5] for example.

### B. Efficient Global Optimization with Kriging and with Co-kriging

Jones in [18], proposed the Efficient Global Optimization (EGO) algorithm. This algorithm can be regarded as a particular case of the optimization-based search formalized in [5] and mentioned in the previous subsection, where the model type is kriging. The infill criterion (choosing the new points of analysis) is to maximize the expected improvement [18,29]. EGO is based on a kriging surrogate model, which starts by interpolating the initial set of data points.

Kriging [34,35] is an interpolating method which features the observed data at all sampling points. The output of a deterministic computer experiment is modeled as a realization of a stochastic process [1,36,37], which is defined as the sum of a global trend function $\mathbf{g}^{\boldsymbol{T}}(\mathbf{x})\beta$ and a Gaussian process $z(\mathbf{x})$ as following

$$\mathrm{y}(\mathbf{x}) = \mathbf{g}^{\boldsymbol{T}}(\mathbf{x})\beta + z(\mathbf{x}) \qquad (3)$$

where $\mathbf{g}(\mathbf{x}) = [g_1(\mathbf{x}), g_2(\mathbf{x}), \dots, g_{\boldsymbol{k}}(\mathbf{x})]^T \in \mathbb{R}^k$ is defined with a set of the regression basis function, $\beta = [\beta_1, \beta_2, \dots, \beta_{\boldsymbol{k}}]^T \in \mathbb{R}^k$ is an unknown vector of regression parameters and $z(\mathbf{x})$ is a zero-mean stationary stochastic process with unknown variance $\sigma^2$ and the covariance

$$R = cov(z(x), z(u)) = \sigma^2 K(x, u) \qquad (4)$$

for some known correlation function $K(\cdot)$. In the application presented in section 5, we consider the popular Gaussian correlation function:

$$K(x, u) = \prod_{k=1}^{np} \exp(-\theta_k |x_k - u_k|^2) \qquad (5)$$

The mean response can be estimated for any untried point $x$ as

$$\widehat{Y_x} = E\{Y_x | Y_s\} = \mathbf{g}_x^T \hat{\beta} + r^T R^{-1}\left(Y_s - F\hat{\beta}\right) \qquad (6)$$

Where $\hat{\beta} = (\mathrm{F}^{\boldsymbol{T}} R^{-\mathbf{1}} \mathrm{F})^{-1} \mathrm{F}^T \mathrm{R}^{-1} Y_s$, $Y_x = y(x)$, F is the matrix of linear equations constructed using the regression function and the experimental design and $Y_s$ is the column vector of length $n_s$, which contains the sample values of the response

The kriging prediction variance can also be estimated by the mean-squared error of the predictor

$$\hat{s}^2(x) = \sigma^2[\,1 + \mathbf{m}^T (F^T R^{-1} F)^{-1}\,\mathbf{m} - r^T \mathrm{R}^{-1}\, r] \qquad (7)$$

where the estimated process variance is $\hat{\sigma}^2 = \frac{(Y_s - F\hat{\beta})^T R^{-1} (Y_s - F\hat{\beta})}{n_s}$ and $\mathbf{m} = \mathrm{F}^T \mathrm{R}^{-1} r - \mathbf{g}$, $r$ is the vector of correlations between the point $u$ and the design of experiment points.

In the present paper we will not only use kriging but also a variant called co-kriging within the surrogate based optimization framework. Co-kriging [28,29] is an approximation model for complex computer codes which is enhanced by data from a cheaper analysis code, under the assumption that the different fidelities of the code are correlated. As Forrester et al. in [28] , we will use here the co-kriging approach with two levels of data (data from expensive simulations and data from cheap simulations). Note that the co-kriging framework can be extended to multiple code levels following the notations used in [27]. We denote $y_e$ the values of the expensive data at points $X_e$, $y_c$ the values of the cheap data at the points $X_c$, $Z_e(.)$ a Gaussian process of the expensive code and $Z_c(.)$ a Gaussian process of the cheap code.

An approximation of the expensive code is given by the cheap code multiplied by a constant scaling $\rho$ plus a Gaussian process $Z_d(.)$, which represents the difference between $Z_e(.)$ and $\rho Z_c(.)$:

$$Z_e(\boldsymbol{x}) = \boldsymbol{\rho} Z_c(.) + Z_d(.) \qquad (8)$$

The co-kriging prediction of the expensive code is given for any untried point $x$ by

$$\widehat{y_e} = \hat{\beta} + cC^{-1}\left(y - \mathbf{1}\hat{\beta}\right) \qquad (9)$$

Where $\hat{\beta} = \frac{\mathbf{1}^T C^{-1} y}{\mathbf{1}^T C^{-1}\mathbf{1}}$, C is the co-kriging covariance matrix, c is the vector of correlations between the point $x$ and the design points and **1** is a column vector of ones,

The estimated mean squared error in the co-kriging prediction is calculated

$$\hat{s}^2(x) = \rho^2 \widehat{\sigma_c}^2 + \widehat{\sigma_d}^2 - c^T C^{-1} c + \frac{1 - \mathbf{1}^T C^{-1} c}{\mathbf{1}^T C^{-1}\mathbf{1}} \qquad (10)$$

where $\widehat{\sigma_c}^2$ is the estimated process variance of the cheap code and $\widehat{\sigma_d}^2$ is the estimated process variance of the difference between the expensive and cheap code. The readers are referred to [[29], chap 8], for a more extensive description.

EGO locates a new point to be sampled by maximizing some metric function *EI*, in order to enrich the design of experiments with points that are likely to perform well in terms of the objective function. This metric is based on the notion of "improvement" that is defined as follows. Let $y_B = \min_{j=1,..,ns} y(x_i)$ be the minimum output that has been evaluated after *ns* runs, we can define the amount of improvement at *x* to be zero if $y(x) \geq y_B$ (i.e $y(x)$ provides no improvement over $y_B$). Similarly if $y(x) < y_B$, the amount of improvement at *x* is defined as $y_B - y(x)$.

We can calculate the expectation of it being an improvement on the best value calculated so far:

$$EI = E[I(x)|Y] =$$

$$= \begin{cases} \left(y_B - \hat{y}(x)\right) \times \xi\left(\frac{y_B - \hat{y}(x)}{\hat{s}(x)}\right) + \hat{s}(x) \times \eta\left(\frac{y_B - \hat{y}(x)}{\hat{s}(x)}\right) & , \hat{s} > 0 \\ 0, \ \hat{s} = 0 \end{cases} \quad (11)$$

where $\xi(.)$ is the cumulative distribution function (CDF), $\eta$ (.) is the probability density function (PDF) of a standard normal distribution and $\hat{y}(x)$ is the kriging or co-kriging predictor at point $x$. EGO iteratively adds points to the data set that maximizes the expected improvement $EI$ located by a global optimization such as a genetic algorithm (GA).

EGO iterates until a stopping criterion is met. Due to high computational cost, it is common to use a maximum number of function evaluations, a maximum allowed CPU time, a maximum number of failed iterative improvement trials as stopping criterion. Another alternative [[29], chap 3] is to set a target value for the expected improvement, meaning the next cycle is only carried out if the expected improvement is above a certain threshold.

### C. Reduced basis modeling.

Model order reduction describes different approaches that aim at significantly decreasing the computational burden associated with the solution of the system of equations Eq. (2) [38,39]. A common approach for model order reduction, denoted as reduced basis approaches (or reduced order modeling by projection), aims at reducing the number of state variables of the model by projection on a certain basis. Accordingly, an approximation of the solution is sought in a smaller subspace V of dimension *m* (with usually *m*<<*n*), while enforcing the residual to be orthogonal to the same sub-space V. Typically, V is defined by a so called *reduced-basis* $\Phi = \{\Phi_1, \ldots, \Phi_m\}$ to be constructed, where $\Phi_i \in \mathbb{R}^n$

The initial problem of Eq. (2) is rewritten, as defined by Galerkin conditions, projected onto the reduced basis:

$$\Phi^T K(\boldsymbol{\mu})\Phi\boldsymbol{\alpha} = \Phi^T \boldsymbol{F} \quad (12)$$

where $\boldsymbol{\alpha}$ are the reduced state variables, that is the coefficients of vector $\boldsymbol{u}$ expressed in the reduced basis $\Phi$, $\boldsymbol{\alpha} \in \mathbb{R}^m$.

At this point it is important to realize that Eq. (12) is equivalent to a reduced order model of the initial problem of Eq. (2). Indeed, solving the problem of Eq. (2) typically involves the inversion of a large system of equations of size *n*, the size of the stiffness matrix $K(\boldsymbol{\mu})$, which for large scale problems can easily reach a size of hundreds of thousands. On the other hand solving the reduced order model of Eq. (12) involves the inversion of a much smaller system of equations of size *m*, the size of the projected stiffness matrix $\Phi^T K(\boldsymbol{\mu})\Phi$, which is

equal to the dimensionality of the reduced basis *m* (typically a few dozen). Solving this reduced order model leads directly to $\boldsymbol{\alpha}$ (given by $\boldsymbol{\alpha} = (\Phi^{\boldsymbol{T}} K(\boldsymbol{\mu})\Phi)^{-\mathbf{1}}\Phi^{\boldsymbol{T}}\boldsymbol{F}$), the coefficients of the solution in the reduced basis.

The problem projected onto the reduced basis thus yields an approximate solution $U_{RB} = \Phi\boldsymbol{\alpha}$ whose accuracy can be quantified by measuring the following error estimator, based on the residual:

$$e_{rb}^2 = \frac{\|K(\boldsymbol{\mu})\Phi\boldsymbol{\alpha} - \boldsymbol{F}\|_2^2}{\|\boldsymbol{F}\|_2^2} \qquad (13)$$

Note that computing this error metric only involves matrix-vector products and differences, its computational cost will thus be negligible compared to solving the full system of equations, especially when the size *n* of the problem increases.

Up to now, the subspace V on which the problem is projected, or more precisely one of its basis Φ, was not specified and many different choices are possible for this projection.

For example, eigenmodes of the operators have been used to reduce numerically the size of the problems for applications in dynamics. These approaches are known as modal analysis, Craig-Bampton [40]. In [41,42] the reuse of Krylov subspaces generated during Krylov iterative solvers was used as a reduced basis. The generalized modes of variables separation techniques (like Proper Generalized Decomposition) can also be used in such a context [43]. Greedy approaches have also been proposed for constructing reduced basis models based on enriching the basis with the sample maximizing the reduced basis error [44].

The Proper Orthogonal Decomposition (POD) can also be a way to build a relevant reduced basis in the context of reduced order modeling by projection [41,45–47]. Indeed, POD [48] (also known as Karhunen Loeve decomposition [49] or principal component analysis [50]) is an approach which consists in constructing a reduced basis from a set of solutions, called snapshots. Mathematically, the extraction of the reduced basis from the snapshots is done by Singular Value Decomposition (SVD) which is relatively stable numerically. Generally, the snapshots are the results of full simulations on a set of points.

In this paper an alternative *on the fly* reduced basis construction method is used. This approach consists in using all the simulations for which the full solution (i.e. the result of the inversion of the full system of Eq. (2)) was computed for constructing the reduced basis. The approach is denoted as *on the fly* since it works all along the optimization process and constructs the reduced basis sequentially as more full solutions become available. Each time a new full solution is available, this solution is first orthonormalized with respect to the already existing vectors of the reduced basis and then added to the basis. Note that our proposed approach is not the same as an SVD on the full set of snapshots, due to the fact that we aim at constructing the basis iteratively *on*

*the fly*. We found that our proposed approach leads to a very similar basis size (to one or two elements close) as applying SVD directly on the full set of snapshots.

Finally, note that, both for the construction of the reduced basis model and for the estimation of the error criterion (Eq. 13) the system matrix $K$ usually needs to be assembled. The assembly time is in general non negligible, however, compared to solving the system once the matrix is assembled, it gets smaller and smaller as the size of the system increases. Furthermore, the assembly can be easily parallelized on multiple cores, with a parallel *for* loop. Alternatively assembly free element-by-element computation of the error estimator is also possible. This means that the reduced basis model can be very efficient at calculating an approximate solution of the problem.

## IV. Reduced basis surrogate based optimization (RBSBO).

### A. General concept

We propose here a framework for coupling surrogate based optimization with reduced basis modeling to significantly reduce the cost of the optimization.

The interest of such a coupling is double. First, not all the points of the initial design of experiments necessarily require to be evaluated using the full simulations. Some points may be computed using a reduced order model, while still maintaining acceptable accuracy. Second, the reduced order models also have high potential of benefiting the infill phase of surrogate based optimization. Indeed the infill points are either close to the predicted optimum, in which case the reduced order model is likely to have good accuracy, since points in immediate vicinity have previously been calculated (using either the full or reduced order models). The other option for infill points is to have them in areas with high potential of improvement, generally areas with sparse points. Due to the sparsity of surrounding points the accuracy of the reduced order calculation at the new infill point may be lower but this is likely to be acceptable since at this type of infill points the first objective is to reduce the variance of the prediction, which can be achieved even with a quite rough approximation. Compared to standard surrogate based optimization our method has the advantage that only a fraction of full numerical model resolutions is required. At the majority of the initial sampling or iteration points, only the inexpensive reduced basis solution needs to be computed.

Fig 1 provides the flowchart of the general process of the proposed procedure.

In the first two steps, after the problem definition, the set of points representing the initial design of experiment is defined. This set of points will serve both for the initial reduced basis extraction as well as for

building the initial surrogate model. A surrogate model is then fitted in step 4 using the response of full and reduced basis simulations. The fitted surrogate model is then used to identify the points where the next simulation needs to be performed (i.e. the next infill point). At that point, the response of the reduced basis model is calculated.

Based on a criterion on the accuracy of the reduced basis model a decision is taken whether to run a full simulation at the next infill point or whether a reduced basis solution is sufficient. Two criteria will be proposed in the next subsections.

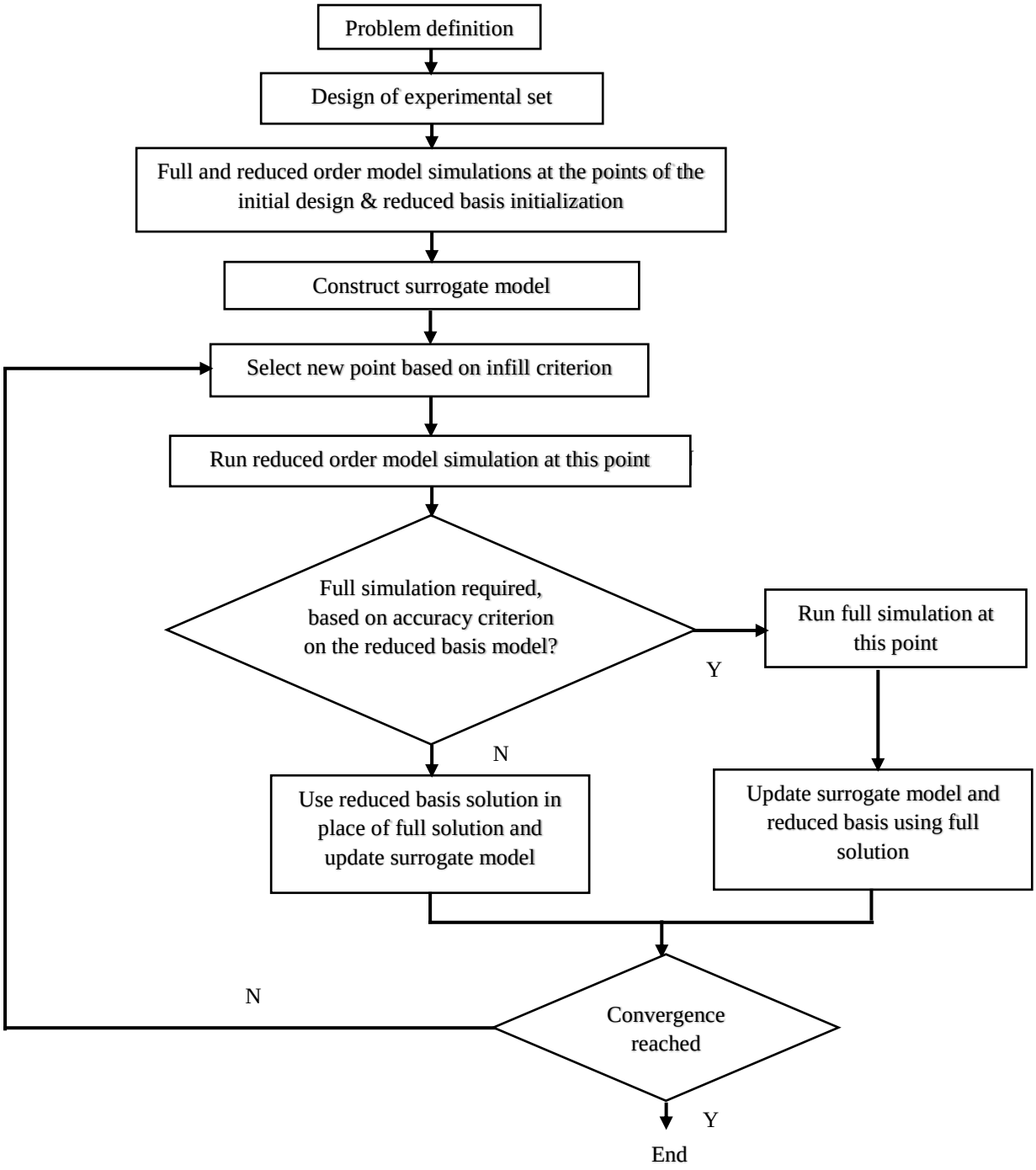


**Fig. 1 Flowchart of the proposed adaptive reduced basis surrogate based optimization**

### B. Key Points Efficient Reduced Basis Global Optimization (KPERBGO)

We propose in this subsection the efficient reduced basis global optimization (KPERBGO) algorithm implementing the framework described above. The proposed algorithm is based on EGO, thus uses kriging as the surrogate model and expected improvement as infill criterion. For the reduced basis construction we chose an approach inspired from [51] called key points approach. This approach allows to sequentially construct a set of points $\mathcal{K}$ which will serve for obtaining the basis vectors. The algorithm of the proposed KPERBGO approach is provided in Algorithm 1 below.

Algorithm 1: KPERBGO Algorithm

1: Create DoE D = $\{\boldsymbol{\mu_i}\}$
2: $\boldsymbol{u} \leftarrow$ solution of $\boldsymbol{K(\mu_1)u = F}$
3: Reduced basis initialization: $\Phi = \boldsymbol{u} / \|\boldsymbol{u}\|_2$
4: $\boldsymbol{Y_{obj}}[\ 1\ ] \leftarrow \boldsymbol{f_{obj}(u; \mu_1)}$
5: **for** $i \in$ remains points of D **do**
6: $\boldsymbol{\alpha} \leftarrow$ solution of $\Phi^T \boldsymbol{K(\mu_i)}\Phi\boldsymbol{\alpha} = \Phi^T \boldsymbol{F}$
7: $\boldsymbol{u} \leftarrow \Phi\boldsymbol{\alpha}$
8: $\boldsymbol{e_{rb}} \leftarrow \|\boldsymbol{K(\mu)}\Phi\boldsymbol{\alpha} - \boldsymbol{F}\|_2 / \|\boldsymbol{F}\|_2$
9: **if** $\boldsymbol{e_{rb}} > \boldsymbol{\varepsilon_{rb}}$ then
10: $\boldsymbol{u} \leftarrow$ solution of $\boldsymbol{K(\mu_i)u = F}$
11: $\boldsymbol{u_{ort}} \leftarrow \boldsymbol{u} - \Phi(\Phi^T \boldsymbol{u})$
12: New key point $\boldsymbol{\mu_i} \in \mathcal{K}$ and reduced basis enrichment: $\Phi \leftarrow \{\Phi,\ \boldsymbol{u_{ort}} / \|\boldsymbol{u_{ort}}\|_2\}$
13: **end if**
14: $\boldsymbol{Y_{obj}}[\ i\ ] \leftarrow \boldsymbol{f_{obj}(u; \mu_i)}$
15: **end for**
16: **while** convergence not reached
17: Fit kriging model to available data (D, $\boldsymbol{Y_{obj}}$)
18: $\boldsymbol{\beta} \leftarrow \boldsymbol{argmax}_{\mu}\ EI(\mu)$
19: $\boldsymbol{\alpha} \leftarrow$ solution of $\Phi^T \boldsymbol{K(\beta)}\Phi\boldsymbol{\alpha} = \Phi^T \boldsymbol{F}$
20: $\boldsymbol{u} \leftarrow \Phi\boldsymbol{\alpha}$
21: $\boldsymbol{e_{rb}} \leftarrow \|\boldsymbol{K(\beta)}\Phi\boldsymbol{\alpha} - \boldsymbol{F}\|_2 / \|\boldsymbol{F}\|_2$
22: **if** $\boldsymbol{e_{rb}} > \boldsymbol{\varepsilon_{rb}}$ then
23: $\boldsymbol{u} \leftarrow$ solution of $\boldsymbol{K(\beta)u = F}$
24: $\boldsymbol{u_{ort}} \leftarrow \boldsymbol{u} - \Phi(\Phi^T \boldsymbol{u})$
25: New key point $\boldsymbol{\beta} \in \mathcal{K}$ and reduced basis enrichment: $\Phi \leftarrow \{\Phi,\ \boldsymbol{u_{ort}} / \|\boldsymbol{u_{ort}}\|_2\}$
26: **end if**
27: D $\leftarrow$ D **U** $\boldsymbol{\beta}$
28: $\boldsymbol{Y_{obj}} \leftarrow \boldsymbol{Y_{obj}}$ **U** $\boldsymbol{f_{obj}(u\ ;\ \beta)}$
29 : **end while**
30: $\boldsymbol{y}^* \leftarrow \min(\boldsymbol{Y_{obj}})$

The algorithm is divided in two main phases. The first one (lines 1-15) corresponds to the construction of the initial kriging model of the objective function. The second one (lines 16-29) corresponds to the iterations for enriching the kriging model and the reduced basis in order to find the global optimum.

For the first phase corresponding to the construction of the initial kriging model the implementation is based on the key points approach [51], which is briefly summarized below.

For the first point, $\boldsymbol{\mu}_1$, of the DoE, the full simulation always needs to be carried out and its result, $\boldsymbol{u}_1$, becomes the first vector of the reduced basis. Then at the point $\boldsymbol{\mu}_i$ it is assumed that one has already a reduced basis of size $m_i$. The problem for parameter $\boldsymbol{\mu}_i$ is then solved by projection on this reduced basis. This corresponds to the inversion of a small system of size $m_i$, whose computational cost is low compared to that of the full simulation. The accuracy of the approximate solution thus constructed is evaluated with a measure of the residual error $e_{rb}$ in Eq. (13). If this indicator is below a certain threshold $\varepsilon_{rb}$, then the quality of the reduced basis solution is considered sufficient and we move on to the next parameter $\boldsymbol{\mu}_{i+1}$. Otherwise, the complete problem is solved for this point and the associated solution is orthogonalized using the Gram-Schmidt orthogonalization as shown in Eq. (14), normalized as shown in Eq. (15) and added to the basis.

$$\Phi_k = u_k - \sum_{i=1}^{k-1} \langle u_k, \Phi_i \rangle \Phi_i \qquad (14)$$

$$\Phi_k = \Phi_k / \|\Phi_k\| \qquad (15)$$

where $\langle .,. \rangle$ denotes the $L^2$ scalar product.

Not that the basis is constructed on the fly, the basis size will thus be determined by the satisfaction of the threshold on the residual error estimator of Eq. (13).

The second phase of Algorithm 1 corresponds to the infill criterion for enriching the model. At each cycle KPERBGO iteratively adds the point β that maximizes the corresponding expected improvement to the DoE. However, unlike traditional EGO, at each additional point β, KPERBGO first uses the reduced order model to calculate the response. If this response meets a prescribed accuracy level, assessed by the residuals error $e_{rb}$ being below a certain threshold $\varepsilon_{rb}$ (see Eq. (13)), then this reduced basis solution is used in place of the full solution. Otherwise (if the response does not meet the prescribed threshold $\varepsilon_{rb}$ on the residuals error $e_{rb}$) the full problem is solved for this point β and the associated solution is orthogonalized as shown in Eq. (14), normalized as shown in Eq. (15) and added to the basis, thus enriching the reduced basis. KPERBGO iterates until a convergence stopping criterion is met.

In the proposed KPERBGO approach, reduced basis solutions are thus used at two different phases: during the evaluation of the responses of the initial design of experiments and during the evaluation of points of the infill phase, that maximize the expected improvement. The KPERBGO approach adaptively choses between using a full simulation or reduced basis one at each step. Since the computational time of the reduced basis solution is significantly lower than that of a full solution, the approach has the potential of major acceleration of the optimization. Note that KPERBGO, like EGO, seeks to make a trade-off between exploration of new areas of the design space and exploitation of the areas near the present best point for determining the global optimum.

The exploration phase is characterized by large model uncertainty thus it is pertinent to use a coarse reduced basis model first in these areas in order to reduce the large kriging model uncertainty. The exploitation phase on the other hand is characterized by a close vicinity to already carried out full simulations, the reduced basis model is thus likely to be quite accurate in this vicinity. Furthermore for both exploration and exploitation in case that the reduced basis model is not sufficiently accurate based on the error estimator of Eq. (13) the proposed approach will run a new full simulation and enrich the reduced basis with this result.

Note also that the KPERBGO approach uses the error metric of Eq. (13) to determine whether a reduced basis solution is sufficient. Based on our experience this error metric will be sufficient for a wide variety of problems, but there may be situations where this may be insufficient, for example for local minima lying far away in the design variable space but extremely close in terms of objective function value.

Finally, note that due to the use of reduced basis models even when close to the optimum, KPERBGO may not be able to converge to the same level as EGO but may be limited to the accuracy of the reduced basis model in the vicinity of the optimum. The examples provided in the application section show that this accuracy is usually sufficient for engineering purposes. Furthermore this algorithm is more efficient in terms of uses of the full solutions. However, in cases where the user needs to precisely control the convergence precision of KPERBGO, we suggest to use the Key Points Efficient Reduced Basis Global Optimization with Terminal Enrichment (KPERBGOTE) described in the next subsection. This algorithm comes at the expense of using a somewhat larger number of full solutions but allows precise convergence control.

### C. Key Points Efficient Reduced Basis Global Optimization with Terminal Enrichment (KPERBGOTE)

To control the convergence precision of KPERBGO, we propose to use full numerical simulation when the next point may be close to the optimum solution. To do that, we use the full model when the response does not meet the prescribed threshold $\varepsilon_{rb}$ on the residuals error $e_{rb}$ or when the next point is located at a certain distance to the best point so far. We call this approach key point Key Points Efficient Reduced Basis Global Optimization with terminal enrichment (KPERBGOTE). In this approach, we define a radius given as follows:

$$R = k * d \qquad (16)$$

where $k$ is a constant given by the user according to the problem to be solved and $d$ represent the distance between the best point so far and its nearest neighbor. Note that k=1 works generally well and this is the value that was used on our problems.

KPERBGOTE proceeds in the following manner: as EGO and KPERBGO, at each cycle, it iteratively adds the point that maximizes the corresponding expected improvement within the DoE. At this point, KPERBGOTE first

checks whether the new point is located inside the ball of radius $R$ in which case the full solution is calculated and used at this point. Otherwise, the reduced order model is evaluated and the algorithm proceeds similarly to KPERBGO by checking if this response meets a prescribed accuracy level, assessed by the residuals error $e_{rb}$ being below a certain threshold $\varepsilon_{rb}$ (see Eq. (13)), in which case the reduced basis solution is used in place of the full solution. If the threshold on the accuracy is not satisfied the full problem is solved for this point and the associated solution is orthogonalized as shown in Eq. (14), normalized as shown in Eq. (15) and added to the basis, thus enriching the reduced basis. KPERBGOTE iterates until a convergence stopping criterion is met.

### D. Key Points Efficient Co-kriging Global Optimization (KPECGO)

In this subsection, we describe the co-kriging version of the proposed approach, that we call Key Points Efficient Co-kriging Global Optimization approach (KPECGO). This approach differs from the KPERBGO approach in two ways.

First, the co-kriging is used in place of kriging. We have two different fidelity models: the high fidelity model represented by the full numerical model and the low fidelity model represented by the reduced order model. After reduced basis initialization, a first initial co-kriging is built based on a design of experiment and key point approach [51]. The point that maximizes the expected improvement is selected, the response of the reduced order model is calculated and the data is added to the data correspond to the cheap code.

Second, unlike in the KPERBGO approach, the criterion used to know if a full model is required is not based on a threshold but based on a quantile defined on the intrinsic error estimate of the co-kriging surrogate. We denote $f_{RB}(x_{new})$ the response of the reduced order model and $d(x_{new})$ the error estimation at $x_{new}$ of the co-kriging model ($d$ being itself modeled by a Gaussian process, see [27,28]), i.e. the estimation of the difference between the full model and the reduced order model. At the point at which the expected improvement is maximum, we calculate an approximation of the expensive code given by $f_{true}(x_{new}) \approx f_{RB}(x_{new}) + d(x_{new})$. Note that since $d(x)$ is a Gaussian process, $f_{true}(x_{new})$ is a normally distributed random variable. If the p-quantile of $f_{true}(x_{new})$ is lower than the best response value so far, the full problem is solved for this point and the data is added to the data corresponding to the expensive code. The co-kriging model is updated using both cheap data and available expensive data. The KPECGO iterates until a convergence stopping criterion is met.

The interpretation of this criterion of using a reduced basis simulation at a given point is that there is a high chance that the true value of the model will be better than the present best point, thus a full simulation is executed at this point. Note that the value $p$ of the quantile can be tuned for a trade-off between increasing

accuracy during the exploration or limiting high accuracy only to the exploitation phase of the infill phase. In the present paper we used the 0.05-quantile ($p$=0.05).

## V. Application to maximum stiffness design of laminated composite plates

Optimum design of composite laminates has been addressed by multiple researchers over the past decades. We refer the reader to the review paper by Venkataraman and Haftka [52] for an overview of some of the topics addressed. In terms of maximum stiffness design (i.e. finding the optimal stacking sequence which maximizes the stiffness of the laminate) the lamination parameters approach [53] has turned out to be a powerful approach allowing to avoid carrying out global optimization directly using expensive finite element models, by decoupling the optimization problem. However, stiffness optimization using the lamination parameters approach has some limitations in handling arbitrary layups as discussed by [54,55]. In particular treating general non-symmetric laminates are still problematic. The present section addresses the problem of maximum stiffness design, first on some benchmark problems, then on general non-symmetric laminates under complex loading.

### A. Description of the problem

In the present section we apply the key point efficient reduced basis global optimization described in section IV.B to stiffness maximization of composite laminates. Minimization of the strain energy $U$, which is equivalent to the criterion of maximum stiffness, is selected as the optimality criterion. The optimization problem is written in the following mathematical form:

$$\begin{aligned} &\min_{\theta} U(\theta) \\ &K\boldsymbol{u} = \boldsymbol{F} \\ &-90 \le \theta_i \le 90\ deg, \quad i = 1,2,\dots,NV \end{aligned} \tag{17}$$

where $\theta$ is the vector of the ply orientations which is explicitly given by $\theta = (\theta_1, \theta_2, \dots, \theta_{NV})^T$ and $NV$ the number of variables. For symmetric ply layups, $NV = NL/2$, where $NL$ the number of layers. In the general case (non-symmetric) $NV$=$NL$. Denoting the assembled structural stiffness matrix as $K$ and the nodal unknowns vector as $\boldsymbol{u}$, the strain energy $U$ is written as:

$$U(\theta) = \frac{1}{2}\boldsymbol{u}^T K \boldsymbol{u} \tag{18}$$

The governing equilibrium equations $K\boldsymbol{u} = \boldsymbol{F}$ are solved with a Matlab based in-house finite element solver. We used four-node Mindlin shell element with five degrees of freedom per node with a shear correction factor computed according to [56]. We consider two possible materials for the laminate, whose ply-elastic constants are provided in Table 1. The two materials considered are representative of high and medium orthotropy composites.

**Table 1. Material properties**

| Parameter | $E_1$(GPa) | $E_2$(GPa) | $\nu_{21}$ | $G_{12}$ (GPa) |
|---|---|---|---|---|
| Material-1 | 181 | 10.3 | 0.28 | 7.17 |
| Material-2 | 260 | 140 | 0.3 | 60 |

### B. Key Point Efficient Reduced Basis Global Optimization implementation

The present subsection provides the implementation of the optimal design of orthotropic structures using the proposed KPERBGO approach.

In the first step, the design of experiments is defined. We use here a Latin hypercube sampling [57] or full factorial design (with different number of samples depending on the size *NV* of the problem) within the bounds $-90 \leq \theta_i \leq 90$ , $i = 1,2, \dots, NV$ where *NV* is the number of variables.

In the second step the key points approach (section IV.B) is applied with an error criterion $e_{rb}$ to construct the initial reduced basis. The algorithm solves exactly the finite element problem with the parameters of the first point of the DoE and adds the solution vector to the basis used for the reduced order modeling. It then solves the second experiment by projection on this basis and checks if the residual error is higher than the considered threshold. Obviously only one vector for the reduced basis is insufficient to capture the variations of the displacement field for this problem. In this case the full problem is solved for experiment 2 and the resulting displacement vector is added to the reduced basis. The approach continues sequentially with the following points until the end of the DoE. Each experiment point is first solved projected on the reduced basis. If the corresponding residual is lower than the considered threshold the algorithm moves to the next DoE point. Otherwise the current point is added to the key points, meaning that the full problem is solved and the reduced basis is enriched by this key point.

The third step consists in fitting a kriging model to the objective function of Eq. (18) and the corresponding output. The point that maximizes the expected improvement is then selected as the next point to be computed. The reduced order model is first used to calculate the response approximation at this point. If the residual measure defined by Eq. (13) is lower than the imposed threshold, the kriging model is updated using this approximate solution. Otherwise, the full numerical solution is calculated at this point and the corresponding output is used to enrich the basis and update the kriging model.

KPERBGO iterates until the maximum number of cycles (simulations including both the full numerical model and reduced order model) is met.

## C. The Key Point Efficient Reduced Basis Global Optimization (KPERBGO) results

The optimal design of orthotropic structures presented in section V.A is now applied on several test problems to compare the performance of the proposed approach.

*1. Symmetric multi-layered laminated plate*

In this subsection we investigate the optimal layups of symmetrically laminated composite plates subject to different loading conditions.

### Simply supported square plate under uniformly distributed pressure loading

To begin with, we consider some test problems for which the optimal solution is known in order to illustrate and compare the capabilities of the method. We consider a square, simply supported plate under a uniformly distributed pressure distribution (cf. Figure 2). We consider symmetric 4, 6 and 8 ply laminates, which respectively involve 2, 3 and 4 design variables. The objective function for the symmetric 4 ply laminate is provided in Figure 3 in terms of the two angles $\theta_1$ and $\theta_2$.

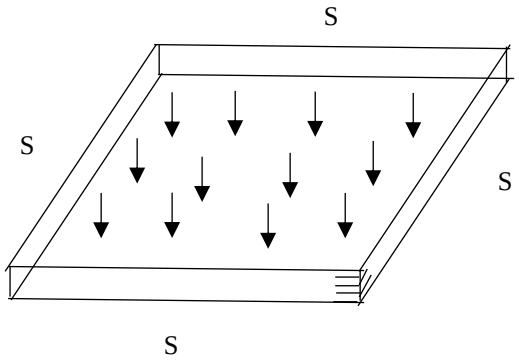


**Figure 2. Laminate under uniformly distributed pressure with simply supported (SS) sides**

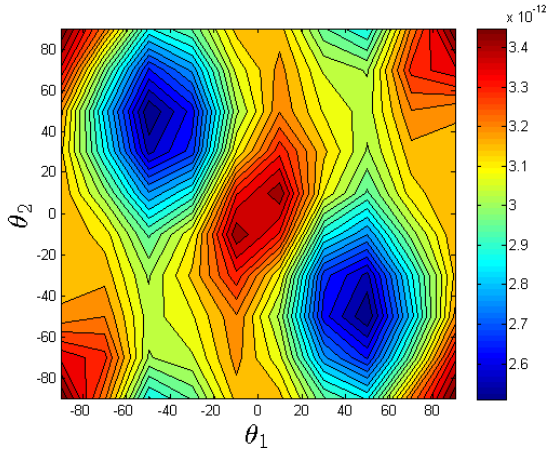


**Figure 3. Contours of the objective function (compliance) for the four-ply symmetric laminate as a function of the two design variables.**

Table 2 provides the optimum layup obtained for the simply supported uniformly distributed problem using different adaptive surrogate model based global optimization approaches. We first provide the reference solution from [58]. We then provide solutions obtained using the EGO and KPERBGO methods (with $e_{rb} = 10^{-3}$ and $10^{-2}$ ). The error compared to the reference solution (given in %) as expressed in Eq. (16) is also provided in Table 2.

$$Err = \frac{f_{obj}^{approx} - f_{obj}^{exact}}{f_{obj}^{exact}} * 100 \qquad (19)$$

where $f_{obj}^{approx}$ represents the kriging approximation value of the objective function (stain energy) at the optimal design and $f_{obj}^{axact}$ represents the true value of the objective function at the optimal design.

**Table 2. Optimum ply arrangement for square, symmetric multi-layered plate (Material-1), simply supported and subject to uniformly distributed pressure loading.**

| | Reference solution [58] | | EGO Results | |
|---|---|---|---|---|
| NL | $\theta^*$ | | $\theta^*$ | Err (Eq. 19) |
| 4 | $[45, -45]_s$ | | $[44{,}9, -45{,}0]_s$ | $2.68*10^{-6}$ |
| 6 | $[45, -45, -45]_s$ | | $[44.9, -45.0, -45.7]_s$ | $2.69*10^{-4}$ |
| 8 | $[45, -45, -45, -45]_s$ | | $[45.2, -44.8, -45.3, -45.2]_s$ | $7.81*10^{-4}$ |
| | KPERBGO ($e_{rb} = 10^{-3}$ ) | | KPERBGO ($e_{rb} = 10^{-2}$ ) | |
| NL | $\theta^*$ | Err | $\theta^*$ | Err (Eq. 19) |
| 4 | $[44.9, -44.9]_s$ | $1.82*10^{-5}$ | $[45.0, -45{,}5]_s$ | $2.57*10^{-3}$ |
| 6 | $[45.2, -45.1, -45.3]_s$ | $1.51*10^{-3}$ | $[44.6, -45.0, -44.7]_s$ | $4.71*10^{-3}$ |
| 8 | $[45.0, -44.5, -45.2, -45.5]_s$ | $1.84*10^{-3}$ | $[45.2, -44.7, -44.8, -45.2]_s$ | $1.91*10^{-3}$ |

The EGO and KPERBGO solutions agree very well with the reference solution in both test cases, i.e. for engineering purposes there is almost no accuracy penalty here for using the reduced basis approach (KPERBGO) compared to the EGO approach that always uses the full solutions.

It is important to note that even though the error in the objective function (Err) is very small there is nevertheless a 1 to 3 orders of magnitude difference between the error of EGO and that of KPERBGO. This difference is due to the reduced basis model that is used, and which allows the KPERBGO algorithm to converge only up to the reduced basis model accuracy in the vicinity of the optimum. In the context of stiffness optimization this accuracy can be considered sufficient for engineering purposes. In case the accuracy is not considered sufficient and the user needs to precisely control the convergence precision, we recommend using the KPERBGOTE algorithm, which includes convergence control, at the expense of slightly more full solutions.

The results of KPERBGOTE applied to this same problem with $e_{rb} = 10^{-3}$ are provided for comparison purposes in Table 3. We can note that using the terminal enrichment we can reach roughly the same convergence as in EGO.

**Table 3. Optimum ply arrangement for square, symmetric multi-layered plate (Material-1), simply supported and subject to uniformly distributed pressure loading with KPERBGOTE**

| Reference Solution | KPERBGOTE ($e_{rb} = 10^{-3}$ ) | |
|---|---|---|
| $\theta^*$ | $\theta^*$ | Err (Eq. 19) |
| $[45, -45]_s$ | $[44.9, -44{,}9]_s$ | $3.19*10^{-6}$ |
| $[45, -45, -45]_s$ | $[44.9, -44.8, -45.2]_s$ | $6.43*10^{-4}$ |
| $[45, -45, -45, -45]_s$ | $[45.1, -45.3, -44.8, -45.0]_s$ | $8.53*10^{-4}$ |

We provide in Table 4 some elements to compare the numerical efficiency of KPERBGO and EGO. The first column provides the number of layers, the second column the number of full systems using EGO and the third and fourth columns the number of reduced order models using KPERBGO (with $e_{rb} = 10^{-3}$ and $e_{rb} = 10^{-2}$ respectively). The fifth and sixth columns provide the size of the reduced basis i.e. the number of full systems using KPERBGO (with $e_{rb} = 10^{-3}$ and $e_{rb} = 10^{-2}$ respectively ). The last two columns provide the ratio of the computational (CPU) time of the EGO algorithm to the computational (CPU) time of the KPERBGO algorithm, i.e. the speedup that was achieved by using the proposed method over the classical EGO approach.

**Table 4. Numerical efficiency comparison of EGO and KPERBGO for square symmetric multi-layered plate, simply supported and uniformly distributed loading.**

| NL | Number of full systems EGO | Number of projected systems, $e_{rb} = 10^{-3}$ KPERBGO | Number of projected systems , $e_{rb} = 10^{-2}$ KPERBGO | Size of reduced basis (full systems KPERBGO), $e_{rb} = 10^{-3}$ | Size of reduced basis (full systems KPERBGO), $e_{rb} = 10^{-2}$ | Computational speed-up, $e_{rb} = 10^{-3}$ | Computational speed-up, $e_{rb} = 10^{-2}$ |
|---|---|---|---|---|---|---|---|
| 4 | 110 | 84 | 98 | 26 | 12 | 3.8 | 8.4 |
| 6 | 160 | 133 | 149 | 27 | 11 | 5.3 | 12.9 |
| 8 | 360 | 335 | 350 | 25 | 10 | 12.4 | 32.7 |

Similarly, we provide in Table 5 the same comparison items for the KPERBGOTE strategy. We note that the accurate convergence control of this strategy had its toll on the number of full simulations, and thus on the efficiency of the method. Depending on the problem under consideration, the user will have to make a choice between accurate convergence control and lower numerical efficiency and more relaxed convergence control but higher efficiency. For the present stiffness optimization we consider that the KPERBGO convergence is sufficient for the relevant engineering purpose and we will use only this algorithm in the subsequent stiffness optimization problems.

**Table 5. Numerical efficiency comparison of the EGO and KPERBGOTE algorithm for a square symmetric multi-layered plate (Material-1), simply supported and uniformly distributed loading**

| NL | Number of full systems EGO | Number of projected systems KPERBGOTE, $e_{rb} = 3$ | Size of the reduced basis (full systems KPERBGOTE), $e_{rb} = 10^{-3}$ | Computational speed-up, $e_{rb} = 10^{-3}$ |
|---|---|---|---|---|
| 4 | 110 | 76 | 34 | 2.9 |
| 6 | 160 | 124 | 36 | 4.0 |
| 8 | 360 | 323 | 37 | 8.8 |

To illustrate further how the KPERBGO approach works, we analyze in Figure 4 the evolution of the residual throughout the optimization process in the case of the eight-ply laminate. A similar analysis can be done for the other ply arrangements. At the beginning of the optimization the residuals are relatively high, meaning that the full numerical solutions need to be calculated. We can explain this behavior by the fact that a minimum basis size is required to have good accuracy of the reduced basis solution. Once this critical basis size is reached the residuals go below the residuals threshold, represented by the red horizontal line in Figure 4, meaning that the reduced basis solution is used in place of the full solution. Throughout the KPERBGO optimization process, at a small number of simulations, the residuals exceed the threshold again implying that the full solutions need to be computed and the reduced basis updated.

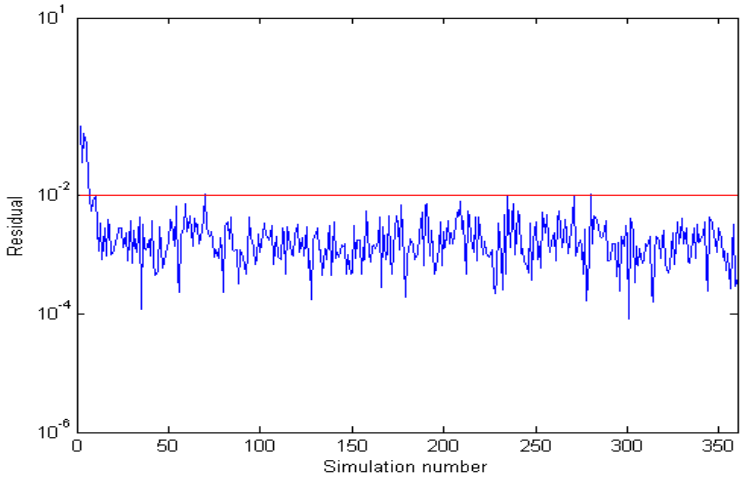


**Figure 4. Plot of the residuals values with the number of simulation for square symmetric eight layered plate, simply supported and uniformly distributed loading with $e_{rb} = 10^{-2}$**

For the EGO algorithm, the simulations consist in computing a full resolution for each experiment of the DoE and the point selected at each infill cycle. For the KPERBGO, only a small number (equal to the size of the reduced basis) of the full numerical solutions are calculated. At the majority of points (number of projected systems), the reduced order model, with negligible computational cost, is used. This leads to significant speed-

ups of the KPERBGO approach over the EGO approach. Note that the KPERBGO, compared to the EGO algorithm, is more efficient with larger size finite element problems since the inversion of the system of equations takes longer. Also note that the total computational time depends not only on the system inversion but also both on the stiffness matrix assembly and on the kriging model construction. The kriging construction and updating time will be relatively small if the number of design variables remains reasonable (less than a dozen). The stiffness matrix assembly can be computationally quite expensive, roughly of the same order as the system solving time. However the assembly is very easy to parallelize on multiple cores with a simple parallel "for" loop, unlike the solving of the system, which would require more complex domain decomposition methods to do so. With parallel assembly the time of the stiffness matrix, assembly quickly becomes negligible compared to the system resolution time.

Replacing the finite element model by a surrogate leads to negligible surrogate evaluation cost so that the entire computational cost lies in the surrogate construction and updating. In our case, using the classical EGO approach the optimization with eight layers required 360 full numerical solutions while using the proposed approach with $e_{rb} = 10^{-2}$ involved only 10 full numerical solutions. At the other points reduced order models were used, thus drastically reducing the computational cost compared to the EGO algorithm.

Note that the computational speed-up provided in Table 5 is based on the CPU time, including any overhead costs compared to considering only the solution of the finite element and reduced basis models. When the size *n* of the finite element problem increases, the overhead cost will tend to zero for reduced basis sizes of up to a few dozen vectors, which is typical of reduced basis solutions for a large variety of problems. With negligible overhead cost, the speed-up would be even greater, equaling the ratio of total solutions over full system solutions.

As a final note we also compare how our proposed approach would compare against an evolutionary global optimization algorithm performed on a static kriging approximation of this problem with and without use of reduced basis modeling. This would be a classic surrogate based approximation framework with the notable distinction that the kriging metamodel is also constructed using reduced basis modeling (see key points approach[51]).

To build the kriging metamodel of the objective function of the four-ply laminate problem, we use a Latin Hypercube Sampling of size 2000. For the optimization we use a differential evolution global optimization proposed by Storn [59]. We obtain $[45.7, -44.8]_s$ as solution with relative error of 0.01% compared to the reference solution (see first column of Table 2). Second we built a static kriging model of the objective function

in conjunction with reduced basis modeling using the key point approach with $e_{rb} = 10^{-3}$. Using the same differential evolution algorithm we obtain $[46.1, -45.2]_s$ as solution with a relative error of 0.03%, 44 full model evaluations and 1974 reduced order model evaluations. We can note that, even though a very large design of experiments was used, the solutions are significantly less converged than using EGO types algorithms (we have a relative error in the objective function which is between one and four orders of magnitude higher here). Indeed for this type of problems EGO allows to be more economical in the choice of points that really need to be executed. While reduced basis modeling using the key points approach allows a significant gain over the traditional kriging construction, the surrogate based evolutionary optimization is still much more greedy for this type of problems than the proposed KPERBGO and KPERBGOTE approaches.

**Plate with hole**

A similar investigation was carried out using a more complex structure and loading conditions, for which no existing solutions could be found by the authors. We considered a plate with a hole, clamped on one side and subject to uniformly distributed pressure on the top and in-plane shear loading on the side opposite to the clamping (cf. Figure 5). We will first consider a symmetric laminate, after which we will investigate the more complex case of a non-symmetric laminate with variable number of plies. Note that in the latter case, the arbitrary stacking sequence (non-symmetric) of the laminate renders the problem quite difficult to solve, in particular preventing the traditional decoupling approach based on lamination parameters [53], that the majority of previous works employed.

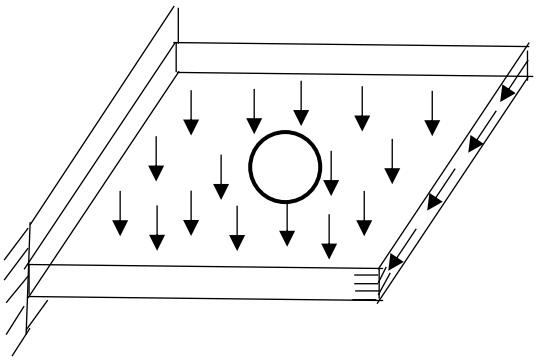

**Figure 5. Boundary conditions and loading for the plate with a hole problem**

To begin with and illustrate graphically the behavior of the proposed approach we start with a low-dimensional problem involving a symmetric plate with four plies (thus involving only two design variables). The corresponding maximum stiffness objective function involves two minima, a local one and a global one (cf. contour plots in Figure 6). Note that the two minima, corresponding to inverting the laminate stacking sequence,

do not have the same objective function value (stiffness) due to the non-symmetry in the loading conditions. The shear loading on the edge, combined with bending-extension coupling due to the non-symmetry of the laminate leads to one of the two minima to have a lower stiffness than the other. Considering the presence of local minima, the problem is thus well suited for being solved by EGO-type algorithms.

Figure 6 shows the first fifty simulations on the test function for both the EGO and KPERBGO approaches. The black circles are the initial samples of 9 points (initial design of experiments) and the red circles the additional points chosen by the expected improvement maximization. The filled circles represent the full numerical solution and the hollow circles the solutions obtained using the reduced order model. For the EGO algorithm (Figure 6.a) all the infill points are full simulations. On the other hand for KPERBGO (Figure 6.b) most of the infill points were calculated with the reduced order model, thus leading to a significant computational cost reduction. The reason why the reduced basis approach works well is that EGO type algorithms have an exploitation phase where the infill points will be clustered around a local or global minimum. For these points, which are quite close to each other, the reduced basis model will tend to work quite well since a full solution was calculated for a point in close vicinity, the solution projected on the reduced basis will thus be sufficiently accurate.

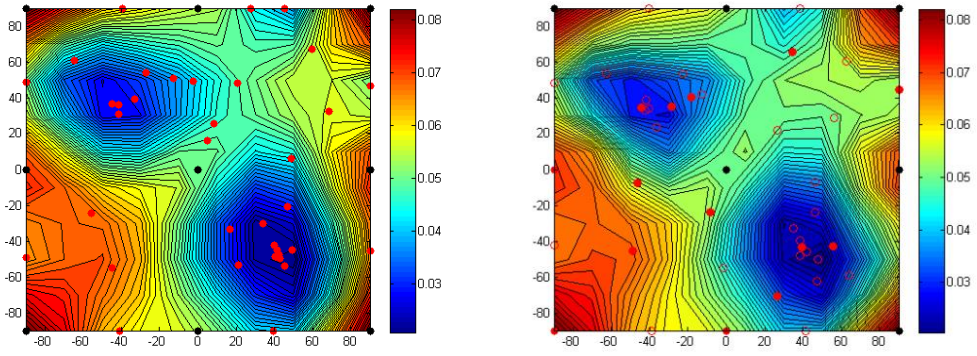


***a) EGO*** ***b) KPERBGO***

**Figure 6. Contours of the kriging objective function with the initial sample (black circles) and the first forty-one points selected by the expected improvement maximization (red circles): a) EGO approach b) the proposed KPERBGO approach with $e_{rb} = 5 * 10^{-2}$. Hollow circles denote reduced basis simulations.**

Tables 6 presents the optimum results for laminates with an increasing number of plies using EGO and KPERBGO with $e_{rb} = 5 * 10^{-2}$. Comparing both the ply layup and the difference in objective function we can note that the KPERBGO solution agrees very well with the EGO solution for any engineering purposes. Note however that both EGO and KPERBGO provide approximate solutions and since we do not know the true optimum it is not possible to validate the approach on this example. KPERBGO would in particularly suffer from the same limitations as EGO in terms of finding the global optimum, thus we do not recommend to apply

the KPERBGO algorithm to problems unsuited for EGO (e.g. high dimensional problems, discontinuous objective functions, etc.). For problems suited for EGO, KPERBGO can however speed-up the solution as shown in Table 7, while remaining very close to the EGO solution. On this test case the solutions, for engineering purposes, are considered equivalent but if one seeks tighter convergence control, one could also apply the KPERGOTE algorithm to the problem.

**Table 6. Optimum ply arrangement for symmetric multi-layered plate with a hole (Material-1)**

| | EGO | KPERBGO ($e_{rb} = 5 * 10^{-2}$ ) | |
|---|---|---|---|
| NL | $\theta^*$ | $\theta^*$ | Err KPERBGO to EGO |
| 4 | $[42.8, -43.2]_s$ | $[42.8, -43,1]_s$ | 0.0052 |
| 6 | $[43.2, -43.2, -65.6]_s$ | $[43.2, -43.3, -65.3]_s$ | 0.0028 |
| 8 | $[44.1, -39.1, -69.5, -69.8]_s$ | $[44.2, -39.2, -69.7, -69.6]_s$ | 0.0184 |

We provide in Table 7 the ratio of the computational times of the EGO algorithm, to the total computational times of KPERBGO. i.e. the speedup that was achieved by using the proposed method over the classical EGO approach.

**Table 7. Numerical efficiency comparison of the EGO and KPERBGO algorithm for a square symmetric multi-layered plate with hole**

| NL | Number of full systems EGO | Number of projected systems KPERBGO, $e_{rb} = 5 * 10^{-2}$ | Size of the reduced basis (full systems KPERBGO), $e_{rb} = 5 * 10^{-2}$ | Computational speed-up, $e_{rb} = 5 * 10^{-2}$ |
|---|---|---|---|---|
| 4 | 160 | 129 | 31 | 4.7 |
| 6 | 310 | 277 | 33 | 8.2 |
| 8 | 550 | 518 | 32 | 15.1 |

In this case, using the classical EGO approach the optimization with eight layers required 550 full numerical solutions while using the proposed approach with $e_{rb} = 5 * 10^{-2}$ involved only 32 full numerical solutions.

The time speedup achieved for the eight layers problem is quite significant. This is again achieved by the proposed approach by computing the full solution for only 32 out of the 550 simulations. At the 518 other simulations only the reduced basis solution is computed.

Note that the number of reduced basis vectors is roughly constant with the increasing number of layers. This is due to the fact that for the current problem the overall laminate anisotropy achieved with the various number of layers is roughly the same, the complexity of solving the problem is thus roughly the same.

*2. Non-symmetric multi-layered laminated plate*

We consider in this sub-section the case of a non-symmetric laminated plate subject to the same loading conditions as given in Figure 5. The non-symmetry of the laminate renders the problem significantly tougher to solve.

We provide in Table 8 the optimum results for the non-symmetric laminated plates with a hole using EGO and KPERBGO with $e_{rb} = 5 * 10^{-2}$. Again we can note that the KPERBGO solutions agree for all relevant engineering purposes very well with the EGO.

**Table 8. Optimum ply arrangement for non-symmetric multi-layered plate with hole (Material-2)**

| | EGO | KPERBGO ($e_{rb} = 5 * 10^{-2}$) | |
|---|---|---|---|
| NL | $\theta^*$ | $\theta^*$ | Err EGO to KPERBGO |
| 2 | $[42.8, -41.1]$ | $[42.7, -41.3]$ | -0.0367 |
| 3 | $[-43.2, 41.5, 42.0]$ | $[-43.2, 41.3, 41.9]$ | -0.0052 |
| 4 | $[43.1, -45.2, 40.9, -44.2]$ | $[42.9, -44.7, 41.1, -44.0]$ | 0.00079 |

Table 9 provides the comparison of the numerical efficiency on this application problem.

**Table 9. Numerical efficiency comparison of the EGO and KPERBGO algorithm for a square non-symmetric multi-layered plate with hole**

| NL | Number of full systems EGO | Number of projected systems KPERBGO, $e_{rb} = 5 * 10^{-2}$ | Size of the reduced basis (full systems KPERBGO), $e_{rb} = 5 * 10^{-2}$ | Computational speed-up, $e_{rb} = 5 * 10^{-2}$ |
|---|---|---|---|---|
| 2 | 235 | 151 | 84 | 2.5 |
| 3 | 410 | 230 | 180 | 2.0 |
| 4 | 540 | 343 | 197 | 2.3 |

The advantage in numerical efficiency of KPERBGO is smaller in this problem compared to the previous one, but it can still reach a factor of almost three. Optimization of arbitrary (non-symmetric) laminates is known however to be a hard problem, which we can confirm here. The reason why significantly more full simulations are required here is that the deformation shapes of non-symmetric laminates have significantly higher variability than those for symmetric laminates. Accordingly more bases vectors are required in order to accurately approximate solutions by projection on a reduced basis.

## VI. Application to orthotropic elastic constants identification

### A. Description of the identification problem

In the present section we apply the methods described in section IV to the problem of identifying the four orthotropic elastic constants of a composite laminate based on full field displacements.

We will use here a simulated experiment of a tensile test on a plate with a hole (similar to the ASTM D 3039 tensile test on a plate with a hole). The laminated plate has a stacking sequence of $[45,-45,0]_s$ and the dimensions are given in Figure 7, with a total plate thickness of 0.96 mm. The applied tensile force is 1200 N. The full field measurement is assumed to take place on the entire 20 x 20 $mm^2$ area of the specimen. No exact analytical solutions exist for expressing the displacement field, so this problem is solved with an in-house finite element solver based on the gmsh open source mesh generator [60].

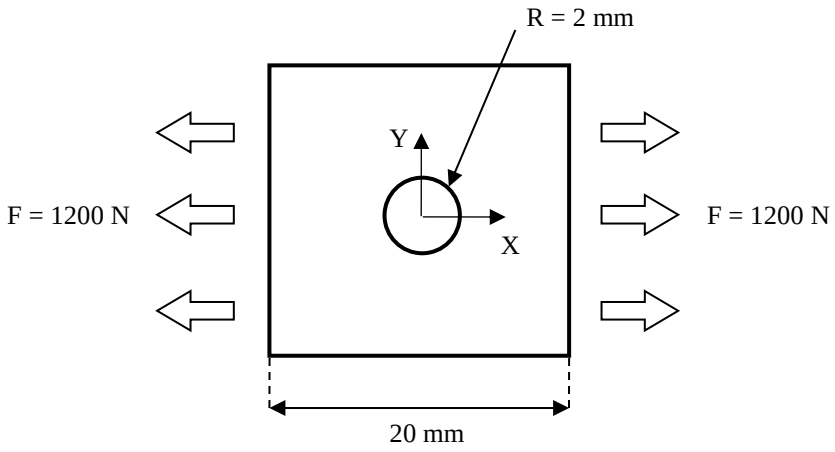


**Figure 7. Simulated experiment specimen geometry and the material orientation axes.**

The identification problem consists in determining the four orthotropic elastic constants $E_1$, $E_2$, $\nu_{21}$ and $G_{12}$ of the composite laminate, given that we measure the displacement fields in the X and Y directions (see Figure 7) over the entire specimen area. Note that the material orientation 1 corresponds to the X direction while the material orientation 2 corresponds to the Y direction.

Since we wanted to test and compare the efficiency of the methods described in section IV within this identification context we chose to use a simulated experiment such as to have reliable reference values for the material properties.

The simulated experiment was obtained by adding a white noise to finite element results that were run with the material properties provided in Table 10. These properties are typical of a graphite/epoxy composite laminate.

**Table 10.Material properties for the simulated experiment**

| Parameter | $E_1$(GPa) | $E_2$(GPa) | $\nu_{21}$ | $G_{12}$ (GPa) |
|---|---|---|---|---|
| Value | 65.2 | 26.2 | 0.314 | 29 |

The noise on the displacement at each of the mesh nodes was assumed to be Gaussian with zero mean and a standard deviation of 5% of the maximum displacement amplitude.

The displacement fields of the simulated experiment are illustrated in Figure 8.

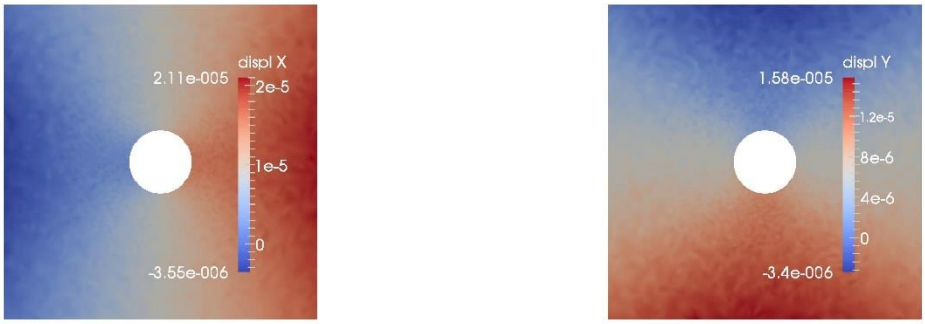


**Figure 8. Displacement fields of the simulated experiment**

The present identification problem is solved in this work using a model updating approach, which involves finding the material properties that minimize the error, expressed in least squares terms, between the model prediction and the measurement represented by the experimental displacement field $U_k^{exp}$. Since this identification formulation involves solving a non linear optimization problem, it is quite sensitive to computational time of the numerical solution.

Accordingly, the objective function is written as:

$$J(E_1, E_2, \nu_{21}, G_{12}) = \frac{1}{2}\left(\sum_{k=1}^{N}\left(U_k(E_1, E_2, \nu_{21}, G_{12}) - U_k^{exp}\right)^2\right) \qquad (20)$$

where N is the size of the displacement field vector (the size of the solution of the finite element problem) and subscript k represents the k-th line of the corresponding vector

The identification formulation is then written as:

$$\min_{\{E_1, E_2, \nu_{21}, G_{12}\}} J$$

**B. The identification problem results**

The identification framework presented in section VI.A is now applied on a test case based on the simulated experiments with a noisy simulation obtained with the material properties given in Table 10, denoted reference values.

The initial design of experiments used is a Latin hypercube design [57] within the bounds provided in Table 11.

**Table 11. Bounds for the design of experiments**

| Parameter | $E_1$(GPa) | $E_2$(GPa) | $\nu_{21}$ | $G_{12}$ (GPa) |
|---|---|---|---|---|
| Lower bound | 50 | 20 | 0.3 | 24 |
| Upper bound | 80 | 32 | 0.35 | 32 |

Based on this DoE the key points approach [51] is applied with an error criterion $e_{rb} = 10^{-3}$ to construct the initial reduced basis.

The identification results are provided in Table 12 with 10426 degrees of freedom.

**Table 12. Identified material properties for the test case**

| Parameter | $E_1$(GPa) | $E_2$(GPa) | $\nu_{21}$ | $G_{12}$ (GPa) | $Err$ (Eq. 19) |
|---|---|---|---|---|---|
| Reference values | 65.2 | 26.2 | 0.314 | 29.000 | 0 |
| EGO | 65.2 | 26.1 | 0.313 | 29.3 | 0.0209 |
| KPERBGO | 65.2 | 26.2 | 0.314 | 29.8 | 0.0695 |
| KPERBGOTE | 65.2 | 26.2 | 0.314 | 28.9 | 0.0278 |
| KPECGO | 65.2 | 26.3 | 0.315 | 29.1 | 0.0069 |

The identified properties generally agree well with the reference values in all test cases.
We provide in Table 13 the ratio of the total computational times (when we use only full simulation) of the EGO algorithm, to the reduced computational times (when we use both full and reduced basis simulations)

**Table 13. Numerical efficiency comparison of the computational cost for the test case**

| Method | Number of systems | Size of the reduced basis (full systems) | Number of projected systems | Computational speed-up |
|---|---|---|---|---|
| EGO | 310 | - | - | - |
| KPERBGO | 310 | 12 | 298 | 23.1 |
| KPERBGOTE | 310 | 15 | 295 | 18.1 |
| KPECGO | 175 | 47 | 128 | 3.27 |

For the EGO algorithm, the simulations consist in computing a full resolution for each experiment of the DoE and the infill points selected at each cycle. For the others approaches, only a fraction of the full numerical solutions is calculated. At the majority of points, the reduced order model, with negligible computational cost is used. The computational speed-up is calculated to indicate the efficiency of the proposed approaches. Note again that reduced basis modeling is more efficient with larger size finite element problems since the inversion of the system of equations takes longer. For very large scale problems significant computational cost savings can thus potentially be achieved.

Note that, while KPECGO achieved the best convergence level with respect to the true optimum and also required the least total number of iterations, it achieved the lowest speed-up through the use of reduced basis. The relatively poor speed-up achieved can be explained by the fact that co-kriging requires a relatively large percentage of high fidelity models in order to merge appropriately the low and high fidelity models. Toal [61]

suggested that between 10% and 80% of the simulations budget should be spent on the low fidelity simulations in order for co-kriging based multifidelity optimization to work well. This of course limits the potential speed-up that can be achieved. Based on these first attempts to use co-kriging within the proposed reduced basis surrogate based optimization framework co-kriging does not appear to bring any significant benefits. This is likely due to the fact that the reduced basis models are for the majority of infill points quite accurate and using the co-kriging is then overkill for trying to fuse simulations of almost same fidelity. Further investigations of co-kriging within a reduced basis framework are left for future work.

## VII. Conclusions

The present article proposed an approach for improving the efficiency of global optimization based on the combination of reduced basis modeling and the efficient global optimization algorithm. The proposed approach seeks to construct an initial reduced basis that requires only a small number of expensive full numerical solutions made possible by an efficient reduced basis method. The full scale (expensive) problem is only solved at a small number of key DoE points, while the reduced order model is used at all the others. The infill phase of the optimization also benefits from running reduced order models, whenever their accuracy is sufficient. Since the infill phase often clusters points in regions of local or global minima, the reduced basis modeling can be particularly efficient since the reduced order model for a point in close vicinity to points that served for the reduced basis construction will often have sufficiently high accuracy. We proposed three different implementations of the general concept exposed.

The efficiency of the proposed coupling approaches is demonstrated on stiffness maximization of laminated composites as well as on the identification of orthotropic elastic constants. Compared to the crude EGO method that required full scale problem solving at each design of experiment point and at all the additional points that maximize the expected improvement, our approach showed great potential to reduce the computational costs. Note that the effectively achievable speed-up is problem dependent. Nevertheless on the application problems, we obtained a speed-up of up to a factor of 32.7.

## Acknowledgements

The authors would like to thank Jean-Charles Passieux for his input on the reduced basis modeling of the identification problem.

## References


[1] Sacks, J., Welch, W. J., Mitchell, T. J., and Wynn, H. P., "Design and Analysis of Computer Experiments," *Statistical Science*, vol. 4, 1989, pp. 409–435.

[2] Kleijnen, J. P. C., Sanchez, S. M., Lucas, T. W., and Cioppa, T. M., "State-of-the-Art Review: A User's Guide to the Brave New World of Designing Simulation Experiments," *INFORMS Journal on Computing*, vol. 17, Aug. 2005, pp. 263–289.

[3] Chen, V. C. P., Tsui, K.-L., Barton, R. R., and Meckesheimer, M., "A review on design, modeling and applications of computer experiments," *IIE Transactions*, vol. 38, 2006, pp. 273–291.

[4] Queipo, N. V., Haftka, R. T., Shyy, W., Goel, T., Vaidyanathan, R., and Kevin Tucker, P., "Surrogate-based analysis and optimization," *Progress in Aerospace Sciences*, vol. 41, Jan. 2005, pp. 1–28.

[5] Forrester, A. I. J., and Keane, A. J., "Recent advances in surrogate-based optimization," *Progress in Aerospace Sciences*, vol. 45, Jan. 2009, pp. 50–79.

[6] Wang, L., Shan, S., and Wang, G. G., "Mode-pursuing sampling method for global optimization on expensive black-box functions," *Engineering Optimization*, vol. 36, Aug. 2004, pp. 419–438.

[7] Sóbester, A., Leary, S. J., and Keane, A. J., "On the Design of Optimization Strategies Based on Global Response Surface Approximation Models," *Journal of Global Optimization*, vol. 33, Sep. 2005, pp. 31–59.

[8] Viana, F. A. C., Simpson, T. W., Balabanov, V., and Toropov, V., "Metamodeling in multidisciplinary design optimization: how far have we really come?," *AIAA Journal*, vol. 52, 2014, pp. 670–690.

[9] Viana, F. A., Gogu, C., and Haftka, R. T., "Making the most out of surrogate models: tricks of the trade," *ASME 2010 International Design Engineering Technical Conferences and Computers and Information in Engineering Conference*, American Society of Mechanical Engineers, 2010, pp. 587–598.

[10] Myers, R., Montgomery, D., Anderson, C., and Anderson-Cook, C., *Response surface methodology: process and product optimization using designed experiments*, Hoboken, New Jersey, USA: John Wiley and Sons, 2009.

[11] Park, J., and Sandberg, I. W., "Universal Approximation using Radial-Basis-Function Networks," *Neural computation*, vol. 3, 1991, pp. 246–257.

[12] Cheng, B., and Titterington, D. M., "Neural networks: A review from a statistical perspective," *Statistical science*, 1994, pp. 2–30.

[13] Goel, T., and Stander, N., "Comparing three error criteria for selecting radial basis function network topology," *Computer Methods in Applied Mechanics and Engineering*, vol. 198, May 2009, pp. 2137–2150.

[14] Boser, B. E., Guyon, I. M., and Vapnik, V. N., "A training algorithm for optimal margin classifiers," *Proceedings of the fifth annual workshop on Computational learning theory*, ACM, 1992, pp. 144–152.

[15] Cortes, C., and Vapnik, V., "Support-vector networks," *Machine learning*, vol. 20, 1995, pp. 273–297.

[16] Müller, K.-R., Mika, S., Rätsch, G., Tsuda, K., and Schölkopf, B., "An introduction to kernel-based learning algorithms," *Neural Networks, IEEE Transactions on*, vol. 12, 2001, pp. 181–201.

[17] Smolas, A. J., and Schölkopf, B., "A tutorial on support vector regression," *Statistics and Computing*, vol. 14, 2004, pp. 199–222.

[18] Jones, D. R., Schonlau, M., and Welch, W. J., "Efficient global optimization of expensive black-box functions," *Journal of Global optimization*, vol. 13, 1998, pp. 455–492.

[19] Huang, D., Allen, T. T., Notz, W. I., and Miller, R. A., "Sequential kriging optimization using multiple-fidelity evaluations," *Structural and Multidisciplinary Optimization*, vol. 32, Sep. 2006, pp. 369–382.

[20] Picheny, V., Ginsbourger, D., Richet, Y., and Caplin, G., "Quantile-based optimization of Noisy Computer Experiments with Tunable Precision," *Technometrics*, vol. 55, 2013, pp. 2–13.

[21] Sen, S., "Reduced-Basis Approximation and A Posteriori Error Estimation for Many-Parameter Heat Conduction Problems," *Numerical Heat Transfer, Part B: Fundamentals*, vol. 54, Oct. 2008, pp. 369–389.

[22] Nguyen, N. C., "A multiscale reduced-basis method for parametrized elliptic partial differential equations with multiple scales," *Journal of Computational Physics*, vol. 227, Dec. 2008, pp. 9807–9822.

[23] Boyaval, S., Bris, C. L., Maday, Y., Nguyen, N. C., and Patera, A. T., "A reduced basis approach for variational problems with stochastic parameters: Application to heat conduction with variable Robin coefficient," *Computer Methods in Applied Mechanics and Engineering*, vol. 198, Sep. 2009, pp. 3187–3206.

[24] Manzoni, A., Quarteroni, A., and Rozza, G., "Shape optimization for viscous flows by reduced basis methods and free-form deformation," *International Journal for Numerical Methods in Fluids*, vol. 70, Oct. 2012, pp. 646–670.

[25] Gogu, C., "Improving the efficiency of large scale topology optimization through on-the-fly reduced order model construction," *International Journal for Numerical Methods in Engineering*, vol. 101, Jan. 2015, pp. 281–304.

[26] Forrester, A. I. J., Bressloff, N. W., and Keane, A. J., "Optimization using surrogate models and partially converged computational fluid dynamics simulations," *Proceedings of the Royal Society A: Mathematical, Physical and Engineering Sciences*, vol. 462, Jul. 2006, pp. 2177–2204.

[27] Kennedy, M. C., and O'Hagan, A., "Predicting the output from a complex computer code when fast approximations are available," *Biometrika*, vol. 87, 2000, pp. 1–13.
[28] Forrester, A. I. J., Sóbester, A., and Keane, A. J., "Multi-fidelity optimization via surrogate modelling," *Proceedings of the Royal Society A: Mathematical, Physical and Engineering Sciences*, vol. 463, Dec. 2007, pp. 3251–3269.
[29] Forrester, A. I. J., Sóbester, A., and Keane, A., *Engineering Design via Surrogate Modelling: A Practical Guide*, John Wiley & Sons, 2008.
[30] Keane, A., and Nair, P., *Computational approaches for aerospace design: the pursuit of excellence*, John Wiley & Sons, 2005.
[31] Wang, G. G., and Shan, S., "Review of Metamodeling Techniques in Support of Engineering Design Optimization," *Journal of Mechanical Design*, vol. 129, 2007, p. 370.
[32] Giunta, A. A., Wojtkiewicz, S. F., and Eldred, M. S., "Overview of modern design of experiments methods for computational simulations," *Proceedings of the 41st AIAA aerospace sciences meeting and exhibit, AIAA-2003-0649*, 2003.
[33] Simpson, T. W., Poplinski, J. D., Koch, P. N., and Allen, J. K., "Metamodels for computer-based engineering design: survey and recommendations," *Engineering with computers*, vol. 17, 2001, pp. 129–150.
[34] Krige, D. G., "A Statistical Approach to Some Basic Mine Valuations Problems on the Witwatersrand," *Journal of the Chemical, Metallurgical and Mining Society of the South Africa*, vol. 52, 1951, pp. 119–139.
[35] Matheron, G., *Le krigeage universel. Cahiers du centre de Morphologie mathématique*, Fontainebleau: 1969.
[36] Stein, M. L., *Interpolation of Spatial Data*, New York, NY: Springer New York, 1999.
[37] Martin, J. D., and Simpson, T. W., "Use of Kriging Models to Approximate Deterministic Computer Models," *AIAA Journal*, vol. 43, 2005, pp. 853–863.
[38] Schilders, W. H. A., van der Vorst, H. A., and Rommes, J., eds., *Model Order Reduction: Theory, Research Aspects and Applications*, Berlin, Heidelberg: Springer Berlin Heidelberg, 2008.
[39] Benner, P., Gugercin, S., and Willcox, K., "A Survey of Model Reduction Methods for Parametric Systems," *MPIMD*, pp. 13–14.
[40] Bampton, M., and Craig, R., "Coupling of substructures for Dynamic Analyses," *AIAA Journal*, vol. 6, 1968, pp. 1313–1319.
[41] Kerfriden, P., Gosselet, P., Adhikari, S., and Bordas, S. P. A., "Bridging proper orthogonal decomposition methods and augmented Newton–Krylov algorithms: An adaptive model order reduction for highly nonlinear mechanical problems," *Computer Methods in Applied Mechanics and Engineering*, vol. 200, Jan. 2011, pp. 850–866.
[42] Gosselet, P., "Méthodes de décomposition de domaine et méthodes d'accélération pour les problèmes multichamps en mécanique non-linéaire," Université Paris 6, 2003.
[43] Ladevèze, P., Passieux, J.-C., and Néron, D., "The LATIN multiscale computational method and the Proper Generalized Decomposition," *Computer Methods in Applied Mechanics and Engineering*, vol. 199, Apr. 2010, pp. 1287–1296.
[44] Grepl, M. A., Maday, Y., Nguyen, N. C., and Patera, A. T., "Efficient reduced-basis treatment of nonaffine and nonlinear partial differential equations," *ESAIM: Mathematical Modelling and Numerical Analysis*, vol. 41, May 2007, pp. 575–605.
[45] Krysl, P., Lall, S., and Marsden, J. E., "Dimensional model reduction in non-linear finite element dynamics of solids and structures," *International Journal for numerical methods in engineering*, vol. 51, 2001, pp. 479–504.
[46] Ryckelynck, D., "A priori hyperreduction method: an adaptive approach," *Journal of Computational Physics*, vol. 202, Jan. 2005, pp. 346–366.
[47] Meng, L., Breitkopf, P., Raghavan, B., Mauvoisin, G., Bartier, O., and Hernot, X., "Identification of material properties using indentation test and shape manifold learning approach," *Computer Methods in Applied Mechanics and Engineering*, vol. 297, Dec. 2015, pp. 239–257.
[48] Kunisch, K., and Volkwein, S., "Galerkin proper orthogonal decomposition methods for a general equation in fluid dynamics," *SIAM Journal on Numerical analysis*, vol. 40, 2002, pp. 492–515.
[49] Karhunen, K., "Uber lineare methoden für wahrscheinigkeitsrechnung," *Annales of Academic Science Fennicae Series A1 Mathematical Physics*, 1943, p. 37:3-79.
[50] Hotteling, H., "Analysis of Complex of statistical variables into principal component," 1993, p. 24:417--441.
[51] Gogu, C., and Passieux, J.-C., "Efficient surrogate construction by combining response surface methodology and reduced order modeling," *Structural and Multidisciplinary Optimization*, vol. 47, 2013, pp. 821–837.
[52] Venkataraman, S., and Haftka, R. T., "Optimization of composite panels-a review," *Proceedings-American Society for Composites*, 1999, pp. 479–488.
[53] Miki, M., and Sugiyamat, O., "Optimum Design of Laminated Composite Plates Using Lamination Parameters," *AIAA Journal*, vol. 31, 1993, pp. 921–922.

[54] Foldager, J., Hansen, J. S., and Olhoff, N., "A general approach forcing convexity of ply angle optimization in composite laminates," *Structural Optimization*, vol. 16, 1998, pp. 201–211.
[55] Setoodeh, S., Abdalla, M. M., and Gürdal, Z., "Design of variable–stiffness laminates using lamination parameters," *Composites Part B: Engineering*, vol. 37, Jun. 2006, pp. 301–309.
[56] Ferreira, A. J. M., *MATLAB Codes for Finite Element Analysis*, 2009.
[57] Mckay, M. D., Beckman, R. J., and Conover, W. J., "A Comparison of Three Methods for Selecting Values of Input Variables in the Analysis of Output From a Computer Code," *Technometrics*, vol. 42, Feb. 2000, pp. 55–61.
[58] Potgieter, E., and Stander, N., "The genetic algorithm applied to stiffness maximization of laminated plates: review and comparison," *Structural optimization*, vol. 15, 1998, pp. 221–229.
[59] Storn, R., and Price, K., "Differential evolution–a simple and efficient heuristic for global optimization over continuous spaces," *Journal of global optimization*, vol. 11, 1997, pp. 341–359.
[60] Geuzaine, C., and Remacle, J.-F., "Gmsh: A 3-D finite element mesh generator with built-in pre-and post-processing facilities," *International Journal for Numerical Methods in Engineering*, vol. 79, 2009, pp. 1309–1331.
[61] Toal, D. J. J., "Some considerations regarding the use of multi-fidelity Kriging in the construction of surrogate models," *Structural and Multidisciplinary Optimization*, vol. 51, Jun. 2015, pp. 1223–1245.